

Can interference patterns in the reflectance spectra of GaN epilayers give important information of carrier concentration?

C. C. Zheng, S. J. Xu, F. Zhang, J. Q. Ning, D. G. Zhao et al.

Citation: *Appl. Phys. Lett.* **101**, 191102 (2012); doi: 10.1063/1.4766188

View online: <http://dx.doi.org/10.1063/1.4766188>

View Table of Contents: <http://apl.aip.org/resource/1/APPLAB/v101/i19>

Published by the [American Institute of Physics](http://www.aip.org).

Related Articles

Correlations between the morphology and emission properties of trench defects in InGaN/GaN quantum wells
J. Appl. Phys. **113**, 073505 (2013)

Optical characterization of free electron concentration in heteroepitaxial InN layers using Fourier transform infrared spectroscopy and a 2×2 transfer-matrix algebra
J. Appl. Phys. **113**, 073502 (2013)

Influence of structural anisotropy to anisotropic electron mobility in a-plane InN
Appl. Phys. Lett. **102**, 061904 (2013)

Temperature dependent carrier dynamics in telecommunication band InAs quantum dots and dashes grown on InP substrates
J. Appl. Phys. **113**, 033506 (2013)

Sub-250nm light emission and optical gain in AlGaIn materials
J. Appl. Phys. **113**, 013106 (2013)

Additional information on *Appl. Phys. Lett.*

Journal Homepage: <http://apl.aip.org/>

Journal Information: http://apl.aip.org/about/about_the_journal

Top downloads: http://apl.aip.org/features/most_downloaded

Information for Authors: <http://apl.aip.org/authors>

ADVERTISEMENT

AIP | Applied Physics
Letters

SURFACES AND INTERFACES
Focusing on physical, chemical, biological, structural, optical, magnetic and electrical properties of surfaces and interfaces, and more...

ENERGY CONVERSION AND STORAGE
Focusing on all aspects of static and dynamic energy conversion, energy storage, photovoltaics, solar fuels, batteries, capacitors, thermoelectrics, and more...

EXPLORE WHAT'S NEW IN APL

SUBMIT YOUR PAPER NOW!

Can interference patterns in the reflectance spectra of GaN epilayers give important information of carrier concentration?

C. C. Zheng,^{1,2} S. J. Xu,^{1,a)} F. Zhang,¹ J. Q. Ning,¹ D. G. Zhao,³ H. Yang,⁴ and C. M. Che²

¹Department of Physics and HKU-CAS Joint Laboratory on New Materials, The University of Hong Kong, Pokfulam Road, Hong Kong, China

²Department of Chemistry, Institute of Molecular Functional Materials, HKU-CAS Joint Laboratory on New Materials, The University of Hong Kong, Pokfulam Road, Hong Kong, China

³State Key Laboratory on Integrated Optoelectronics, Institute of Semiconductors, Chinese Academy of Sciences, Beijing 100083, China

⁴Suzhou Institute of Nano-tech and Nano-bionics, Chinese Academy of Sciences, Suzhou 215123, China

(Received 5 July 2012; accepted 22 October 2012; published online 6 November 2012)

Low-temperature reflectance spectra of a series of Si-doped GaN epilayers with different doping concentrations grown on sapphire by metal-organic chemical vapour deposition were measured. In addition to the excitonic polariton resonance structures at the band edge, interference oscillating patterns were observed in the energy region well below the band gap. The amplitudes of these oscillation patterns show a distinct dependence on the doping concentrations of the samples. From the thin-film optical interference principle, an approach connecting the amplitude of the interference oscillations and the impurity scattering was established. Good agreement between experiment and theory is achieved. © 2012 American Institute of Physics. [<http://dx.doi.org/10.1063/1.4766188>]

Gallium nitride (GaN) could be the most technologically important material for fabrication of emerging solid-state lighting devices. It has been extensively investigated in the past decades.^{1,2} Usually, GaN epilayers are grown on foreign substrates such as sapphire with advanced thin-film epitaxy techniques due to the lack of large size native substrates. Some nondestructive optical techniques such as photoluminescence and reflectance spectroscopy are frequently employed to investigate the optical properties of GaN epilayers and/or judge the quality of epilayers.^{3–5} In particular, the optical reflectance measurements have been conducted to make *in situ* monitoring the growth status of GaN epilayers.^{6–8} Interference patterns or oscillation structures are commonly observed in these optical reflectance measurements. Such interference patterns certainly carry important information of impurity/defect scattering and even carrier concentration in the epilayers. How to dig out this useful information from the measured oscillation structures in the reflectance spectra is clearly desirable for the growth and quality justification of GaN and other functional epilayers. In this letter, we attempt to link the interference patterns in reflectance spectrum of epilayer with the impurity/defect scattering in the epilayer by proposing a theoretical model based on the general thin-film optical interference principle. By applying this approach to the simulation of the interference patterns observed in reflectance spectra of an undoped GaN and a series of Si-doped GaN epilayers below the fundamental band gap of GaN, we show that the amplitude of the oscillation structures is exponentially dependent on the impurity/defect scattering in the epilayers within low to moderate doping range.

Five GaN epilayers with different Si-doping levels grown on c-sapphire planes using metal-organic chemical vapour deposition (MOCVD), namely MA, MB, MC, MD,

and ME, were investigated in this work. The thickness of all the epilayers is $\sim 4 \mu\text{m}$. MA is intentionally undoped while MB, MC, MD, and ME are doped with the flow rate of silane (SiH_4) at 0.012, 0.025, 0.05, and 0.1 ml/min, respectively, during the growth process. Room-temperature Hall measurements show that the carrier concentrations of MA, MB, MC, MD, and ME were 5.02×10^{15} , 1.52×10^{16} , 6.18×10^{16} , 8.82×10^{16} , and $1.81 \times 10^{17} \text{ cm}^{-3}$, respectively, and the room-temperature Hall mobility of MA, MB, MC, MD, and ME were 48, 930, 852, 841, and $677 \text{ cm}^2 \text{ V}^{-1} \text{ s}^{-1}$, respectively. In the reflectance spectrum measurements, the samples were mounted on the cold finger of a cryostat (Janis, CCS-150) with a varying temperature range from 10 K to 300 K. A high-pressure Xenon arc lamp (XBO 450 W/1 VS1 OSRAM) was employed as the light source. The monochromatic light was achieved by dispersing the white light of the Xenon lamp with an Acton SP305 monochromator equipped with a 1200 lines/mm grating, which was near normally incident on the samples. The reflectance signals from the samples were detected with a Hamamatsu Si p-i-n photodiode and were collected by adopting standard lock-in amplifier technique to enhance the signal-to-noise ratio.

A representative reflectance spectrum (solid line + solid circles) of sample MA at 10 K is shown in Fig. 1. Reflectance spectra of the remaining samples show similar spectral features with that of MA. From Fig. 1, the whole reflectance spectrum can be divided into two distinct spectral regions: the excitonic polariton resonance region at the band-edge⁴ (around 3.5 eV) and the interference oscillation region well below the fundamental band gap. The excitonic polariton resonance structures can be well simulated by an interacting excitonic polariton model considering the two coupled polaritons associated with free exciton A and B, respectively.^{4,9,10} A representative simulation curve (solid line) was also shown in Fig. 1. Detailed simulation and discussion have been published elsewhere.^{4,10} Here, we concentrate on the interference region that is marked out in Fig. 1, which is far

^{a)} Author to whom correspondence should be addressed. Electronic mail: sjxu@hku.hk.

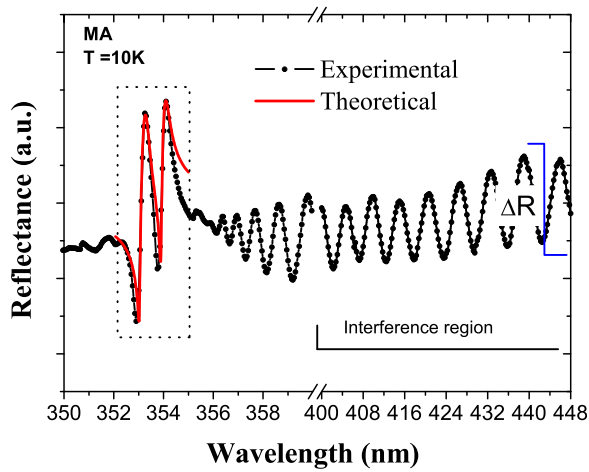


FIG. 1. The low-temperature reflectance spectrum (solid line plus solid circles) of sample MA. The interference region and its amplitude were marked. A simulation curve (solid line) to the reflectance structures of the excitonic polaritons with the interacting excitonic polariton model was also shown. The excitonic polariton resonance region was also marked out by a dotted rectangle.

away from the excitonic resonance region. Figure 2 shows the interference oscillating curves (open symbols) of different samples in the region well below the fundamental band gap. The solid lines are the fitting curves with the model developed in the present study and described in detail later. As seen from Fig. 2, the interference oscillating curves of different GaN epilayers with different Si doping concentrations and almost identical thickness ($\sim 4 \mu\text{m}$) show almost the same oscillation period but different amplitudes and phases. The noticeable difference in both the oscillation amplitude and the phase for different samples clearly reflects a fact that the transmitted light within the epilayers experiences very different impurity/defect scattering since the scattering of light by the GaN epilayer surfaces and the GaN-sapphire interfaces can be reasonably assumed to be equal in all the samples grown under almost the same condition except the doping concentration. Following this idea and starting from the general thin-film optical interference principle, we develop a simple but effective theoretical model to interpret the experimental curves quantitatively, and thus

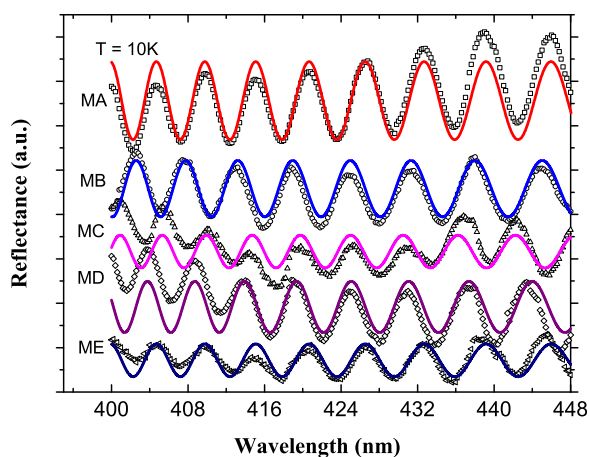


FIG. 2. The measured interference curves (open symbols) of sample MA, MB, MC, MD, and ME at 10 K. The solid lines are the simulating results by using the theoretical model developed in this study.

pave a way to get information of the impurity/defect scattering and even carrier concentration from the interference part of reflectance spectrum of the epilayer.

It starts from a reasonable assumption that the oscillation structure in the longer wavelength region of the reflectance spectrum is mainly caused by the multiple reflecting beam interference, principally illustrated in Fig. 3. Since the intensity of the third and afterward reflected light R_2 and R_i ($i > 2$) is much lower than the first two, namely R_0 and R_1 , it is thus very reasonable for one to consider only two beam interference. Under these assumption and conditions, the superpositioning wave of the two reflected light parts can be written as¹¹

$$R(\lambda) = R_0 + R_1 + 2\sqrt{R_0 R_1} \cos \delta, \quad (1)$$

where λ is the wavelength of incident monochromatic light, $\delta = \frac{4\pi d n_1(\lambda) \cos \theta_1}{\lambda} \pm \pi$ is the phase difference of R_0 and R_1 (π is the phase shift due to surface reflection), $n_1(\lambda)$ is the wavelength dependent refractive index of epilayer (thin film), and θ_1 is the angel of transmitted light from the normal line. Because the interference occurs in the spectral regions well below the fundamental band gap of GaN, the band-edge excitonic absorption induced attenuation of the transmitted light within the GaN epilayers can be neglected.¹² On the other hand, impurity/defect scattering is taken into account as a major factor causing the intensity attenuation of the transmitted light R_1 . In order to consider this loss, we introduce a loss factor, namely γ . Then, Eq. (1) can be modified as

$$R(\lambda) = R_0 + R_1 e^{-\gamma} + 2\sqrt{R_0 R_1} e^{-\gamma/2} \cos \delta. \quad (2)$$

The factor γ is clearly associated with the doping concentrations in the epilayers.

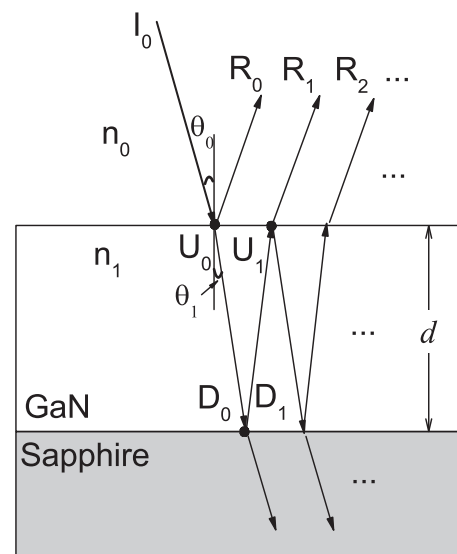


FIG. 3. A schematic diagram of the interference process between GaN surface and GaN/sapphire interface. I, R, U, and D (with corresponding footnotes) stand for the incident, reflected/transmitted waves as noted in the figure. θ_1 and θ_2 represent the incident and transmitted angles, and n_0 ($=1$) and n_1 represent the refractive index in vacuum and GaN, respectively, while d denotes the GaN epilayer thickness.

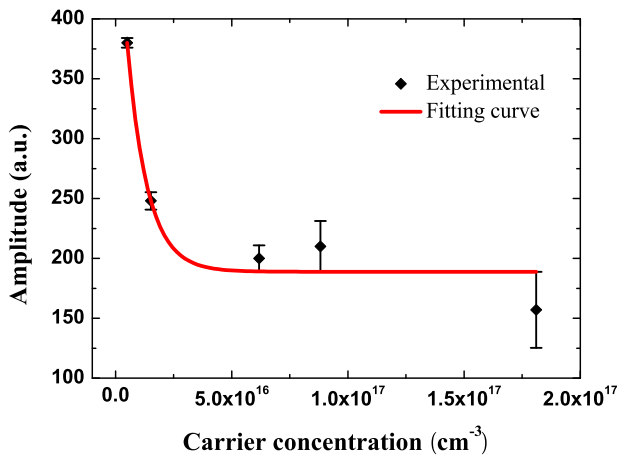


FIG. 4. The amplitude of the interference patterns (solid diamonds) versus the measured Hall carrier concentration of the samples. A first-order exponential decay fitting curve (solid line) is also given.

By adopting the Sellmeier dispersion relationship of refractive index¹³

$$n_1(\lambda)^2 = A^2 + \frac{B^2}{\lambda^2 - C^2}, \quad (3)$$

in which $A = 2.27$, $B = 304.7$ nm, and $C = 294.0$ nm, the reflectance spectra of GaN in the spectral region well below the band gap can be reproduced by combining Eqs. (2) and (3). The fitting curves to the experimental spectra of different samples are depicted as the solid lines in Fig. 2. Constant baselines were adopted to subtract the backgrounds in the fittings for sample MA, MB, MD, and ME, while a sloping line was employed for sample MC. Good agreement between the experimental results and the theoretical curves was achieved. The amplitudes of the interference patterns extracted from fittings are shown in Fig. 4 with the solid symbols against the measured Hall carrier concentration. Clearly, the amplitudes of the interference patterns in the reflectance spectra of different samples show a very sensitive dependence on the doping concentration within a low to moderate doping range, which can be well fitted with a first-order exponential decay function as shown in a solid line in Fig. 4. In fact, under the low temperature condition (i.e., $T \rightarrow 0$), the carrier concentration in Si-doped GaN can be expressed as¹⁴

$$N_c = \frac{N_D}{2 + e^{-\frac{E_c - E_F}{k_B T}}}, \quad (4)$$

where E_c is the energy at the bottom of the conduction band, E_F is the Fermi energy, N_D is the donor concentration which is equal to the Si doping concentration, and k_B is the Boltzmann constant. From Eq. (4), we can see that the carrier concentration is basically proportional to the doping concentration at low temperature. For the influence of possible acceptors or acceptor-like defects in the samples, it can be safely neglected due to their low concentration which is clearly indicated by the extremely weak acceptor related exci-

tonic emission line in the low temperature photoluminescence spectra of the samples (results not shown here). Therefore, at low temperatures (i.e., 10 K adopted in the present study), the carrier concentrations in the GaN epilayers can be reasonably thought to be linearly dependent on the Si doping concentrations. This is why the amplitudes of the oscillation parts in the measured reflectance spectrum show an exponential decay on the carrier concentrations in the epilayers. It should be mentioned that the amplitude of the interference pattern quickly attenuates and tends to reach a constant when the carrier density goes above $\sim 6.18 \times 10^{16} \text{ cm}^{-3}$ in Fig. 4. This can be understandably explained by Eq. (2). On the right side of this equation, a constant term (i.e., the first term) and two exponential decay terms (i.e., the second and third ones) appear.

In summary, the interference patterns in the low-temperature reflectance spectra of the intentionally undoped GaN and a series of Si-doped GaN epilayers grown on sapphire by MOCVD were examined in depth. A theoretical model taking into account the impurity/defect scattering induced light loss in the epilayers was developed to reproduce the interference curves. The results show that the interference patterns in the longer wavelength region and the theoretical approach can be jointly employed to dig out important information of the impurity/defect scattering and even carrier concentration in GaN or other epilayers.

This work was supported by the Joint Research Fund for Overseas Chinese, Hong Kong and Macau Scientists of NSFC (Grant No. 60028012) and the HKU matching fund, the HK-RGC GRF (Grant No. HKU705812), and partially by a grant from the University Grants Committee Areas of Excellence Scheme of the Hong Kong Special Administrative Region, China (Project No. [AoE/P-03/08]).

- ¹H. Morkoç, *Nitride Semiconductors and Devices* (Springer, Berlin, 1999).
- ²S. Nakamura, G. Fasol, and S. J. Pearton, *The Blue Laser Diodes* (Springer, Berlin, 2000).
- ³M. A. Reshchikov and H. Morkoç, *J. Appl. Phys.* **97**, 061301 (2005).
- ⁴Y. J. Wang, R. X. Wang, G. Q. Li, and S. J. Xu, *J. Appl. Phys.* **106**, 013514 (2009).
- ⁵F. Zhang, S. J. Xu, J. Q. Ning, C. C. Zheng, D. G. Zhao, H. Yang, and C. M. Che, *J. Appl. Phys.* **108**, 116103 (2010).
- ⁶Y. T. Hou, Z. C. Feng, S. J. Chua, M. F. Li, N. Akutsu, and K. Matsumoto, *Appl. Phys. Lett.* **75**, 3117 (1999).
- ⁷Z. C. Feng, Y. T. Hou, M. F. Li, S. J. Chua, W. Wang, and L. Zhu, *Phys. Status Solidi B* **216**, 577 (1999).
- ⁸Y. Kobayashi, T. Akasaka, and N. Kobayashi, *J. Cryst. Growth* **195**, 187 (1998).
- ⁹J. Ligois, *Phys. Rev. B* **16**, 1699 (1977).
- ¹⁰C. C. Zheng, S. J. Xu, J. Q. Ning, Y. N. Chen, F. Zhang, and C. M. Che, *Appl. Phys. Lett.* **100**, 221105 (2012).
- ¹¹M. Born and E. Wolf, *Principles of Optics*, 7th ed. (Cambridge University, Cambridge, 1999).
- ¹²J. F. Muth, J. H. Lee, I. K. Shmagin, R. M. Kolbas, H. C. Casey, B. P. Keller, U. K. Mishra, and S. P. DenBaars, *Appl. Phys. Lett.* **71**, 2572 (1997).
- ¹³G. Yu, G. Wang, H. Ishikawa, M. Umeno, T. Soga, T. Egawa, J. Watanabe, and T. Jimbo, *Appl. Phys. Lett.* **70**, 3209 (1997).
- ¹⁴E. K. Liu, B. S. Zhu, and J. S. Luo, *Semiconductor Physics*, 4th ed. (National Defense Industry, Beijing, 1994), p. 63 (in Chinese).